Nonhomologous chromosomal integration of foreign DNA is completely dependent on MUS-53 (human Lig4 homolog) in *Neurospora*

Kazuma Ishibashi, Keiichiro Suzuki, Yoshinori Ando, Chihiro Takakura, and Hirokazu Inoue*

Laboratory of Genetics, Department of Regulation Biology, Faculty of Science, Saitama University, Shimo-okubo 255, Sakura-ku, Saitama 338-8570, Japan

Edited by David D. Perkins, Stanford University, Stanford, CA, and approved August 14, 2006 (received for review May 31, 2006)

Homologous integration of a foreign DNA segment into a chromosomal target sequence enables precise disruption or replacement of genes of interest and provides an effective means to analyze gene function. However, integration after transformation is predominantly nonhomologous in most species other than yeast. Here, we show that homologous integration in the filamentous fungus *Neurospora* requires the homologous-recombination proteins MEI-3 (yeast Rad51 homolog) and MUS-25 (yeast Rad54 homolog), whereas nonhomologous integration requires nonhomologous end-joining protein MUS-52 (yeast Ku80 homolog). Two additional minor integration pathways are present, one MEI-3-independent and homologous, the other MUS-52-independent and nonhomologous. Homologous and nonhomologous mechanisms compete when external DNA is integrated. In *Neurospora*, both nonhomologous integration pathways, MUS-52-dependent and MUS-52-independent, require MUS-53 (a homolog of human Lig4), which functions in the final step of nonhomologous end-joining. Because nonhomologous integration is eliminated in a *LIG4*-disrupted strain, integration occurs only at the targeted site in *mus-53* mutants, making them an extremely efficient and safe host for gene targeting.

homologous integration | *LIG4* | *Neurospora crassa* | gene targeting

DNA double-strand breaks (DSBs) are among the most detrimental DNA lesions. Two major recombination pathways have been identified for their repair (1). These pathways differ as to whether they require DNA sequence homology. Homologous recombination (HR) repairs DSBs by retrieving genetic information from an undamaged homolog, whereas nonhomologous end-joining (NHEJ) rejoins them by direct ligation of the strand ends without any requirement for sequence homology.

These repair mechanisms have been conserved through evolution and operate in a wide range of organisms. Proteins required for HR include Rad51, Rad52, Rad54, and RPA, whereas proteins which are involved in NHEJ include DNA-dependent protein kinase catalytic subunit (DNA-PKcs), the Ku70–Ku80 heterodimer, and the DNA ligase IV (Lig4)–Xrcc4 complex (2). DNA ligase IV is thought to be specific for NHEJ (3–5). The yeast *Saccharomyces cerevisiae* uses mainly the HR system for DSB repair. Therefore, in conventional gene targeting that occurs through the HR mechanism, *S. cerevisiae* shows a very high homologous integration (HI) rate. In contrast with yeast, many other organisms, including mammals, plants, and insects, seem to use NHEJ preferentially for DSB repair. As a result, exogenous DNA can be integrated anywhere in the chromosomes, even if it carries a long stretch of homologous sequence. Therefore, gene targeting is an inefficient method in most species other than yeast.

In humans, the technology of gene targeting through HR is regarded as a potential tool for gene therapy. Although various viral and nonviral vectors have been tried for gene targeting in mammalian cells, the introduced DNA was found to be integrated anywhere in the genome. In gene therapy it has become clear that random, nonhomologous integration (NHI) can activate protooncogenes in patients (6, 7). Therefore, attention is focused on what can be done to minimize the risks of insertional mutagenesis. However, the mechanism of nonhomologous integration, which probably involves the NHEJ pathway, has not yet been clarified.

The filamentous fungus *Neurospora crassa* has been used extensively for studying DNA repair. Genetic and molecular analyses of *Neurospora* mutants revealed that *mei-3*, *mus-11*, and *mus-25* (homologs of *S. cerevisiae RAD51*, *RAD52*, and *RAD54*, respectively) are involved in HR (8–10). Our previous report (11) demonstrated that *mus-51* and *mus-52* (homologs of *S. cerevisiae YKU70* and *YKU80*, which are homologs of human *KU70* and *KU80*, respectively) are involved in NHEJ of *N. crassa*. We also showed that gene targeting rates in *mus-51* and *mus-52* were as high as 100%, compared with ~20% in wild type. This finding was technically important because specific genes can be inactivated very easily if these strains are used as recipients for transformation. These strains have been used in the development of a high-throughput method for knocking out genes of unknown function in *N. crassa* (12). Highly efficient gene targeting has also been reported in *KU*-deficient mutants of *Aspergillus nidulans*, *A. fumigatus*, *A. sojae*, *A. oryzae*, and *Cryptococcus neoformans* (13–17), confirming that *KU*-deficient strains are excellent tools for gene targeting in filamentous fungi. NHEJ components other than *KU70* and *KU80* homologs have not been identified in filamentous fungi. These include homologs of *LIG4* and *XRCC4*.

Here, to investigate the mechanism of gene targeting and chromosomal integration, we measured the chromosomal integration frequency and gene-targeting rate of exogenous DNA in *Neurospora* strains that are defective in HR and NHEJ. Our results suggest that chromosomal integration is achieved by four pathways: two involving MEI-3-dependent and MEI-3-independent HI and two involving MUS-52-dependent and MUS-52-independent NHI. Furthermore, the *Neurospora LIG4*-homolog, *mus-53*, was identified and characterized. Gene targeting in *mus-53* was 100%, the same as in *mus-51* and *mus-52* mutants. However, unlike *mus-51* and *mus-52*, the *mus-53* mutant has a gene-targeting rate of 100% even if the DNA sequence homologous to the targeted is very short. We propose that MUS-53 is required for both the MUS-52-dependent and MUS-52-independent NHI pathways.

Author contributions: K.I. and K.S. contributed equally to this work; K.S. and H.I. designed research; K.I., K.S., Y.A., and C.T. performed research; K.I., K.S., and H.I. analyzed data; and K.S. and H.I. wrote the paper.

The authors declare no conflict of interest.

This paper was submitted directly (Track II) to the PNAS office.

Abbreviations: HI, homologous integration; NHI, nonhomologous integration; HR, homologous recombination; NHEJ, nonhomologous end-joining; DSBs, DNA double-strand breaks; MMS, methyl methanesulfonate; PFP, *p*-fluorophenylalanine.

Data deposition: The sequence reported in this paper has been deposited in the GenBank database (accession no. AB261106).

*To whom correspondence should be addressed. E-mail: hinoue@post.saitama-u.ac.jp.

GENETICS

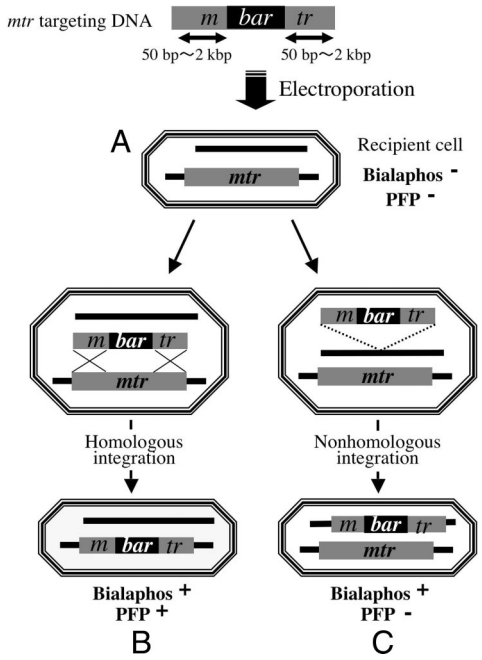

Fig. 1. Scheme of experiments to assay chromosomal integration and targeting efficiency. The black box represents the selectable marker, the bialaphos-resistance gene *bar*. The gray box shows the *mtr* gene. The targeting vector was constructed by replacing part of the *mtr* ORF with *bar*. The *mtr* targeting DNA was flanked by homologous sequences ranging from 50 bp to 2 kbp. Targeting DNA was introduced by electroporation into recipient cells, which are sensitive to both bialaphos and PFP (*A*). Integration into *mtr* by HI results in resistance to both bialaphos and PFP (*B*). NHI produced transformants resistant to bialaphos but sensitive to PFP, because the endogenous *mtr* gene is intact and the *mtr* mutation is recessive (*C*). Integration efficiency was calculated as number of bialaphos-resistant cells per total recipient cell number [(B + C)/A]. The targeting (HI) rate of *mtr* was calculated as the ratio of PFP-resistant transformants to bialaphos-resistant transformants [B/(B + C)], and the NHI rate was calculated as the ratio of PFP-sensitive transformants to bialaphos-resistant transformants [C/(B + C)].

These findings provide new insight into the chromosomal integration mechanisms. *mus-53* also provides a highly efficient alternative to *mus-51* or *mus-52* for inactivating specific genes.

Results

Experimental System to Assay Efficiency. To study the mechanism of foreign DNA integration, we measured the targeting frequency in wild type, in HR-defective strains (*mei-3*, *mus-11*, and *mus-25*), and in the NHEJ-defective strain *mus-52*. Double mutants carrying *mus-52* in combination with each of the HR-defective mutations were also tested to examine the detailed relationships between HR and NHEJ in chromosomal integration. The *mtr* gene on chromosome IV was selected as a target for gene disruption because *mtr*-defective mutants show resistance to the amino acid analog *p*-fluorophenylalanine (PFP) (18). If a DNA fragment including the bialaphos-resistance gene *bar* is integrated at the *mtr* locus, the strain should be resistant to both bialaphos and PFP. On the other hand, if the fragment is integrated at a site other than *mtr*, the strain should be resistant to bialaphos but not to PFP (Fig. 1). Transformation (chromosomal integration) frequencies were calculated as the number of bialaphos-resistant colonies per total recipient cell numbers. The HI rate (gene targeting) was calculated as the ratio of PFP-resistant transformants to bialaphos-resistant transformants. The NHI rate (nonhomologous chromosomal integration) is the ratio of PFP-sensitive transformants to bialaphos-resistant transformants. We constructed linear DNA fragments with long (2-kbp) or short (50-bp) sequences showing homology for the *mtr* region carried on each side of the *bar* gene. These fragments were introduced by electroporation into recipient strains with different genetic backgrounds.

Four Independent Pathways for Integrating Foreign DNA into *N. crassa* Chromosomes. The HI rate was 23.33% in wild-type but 0% in HR-defective strains, including *mei-3*, *mus-11*, and *mus-25* (Table 1). This result clearly demonstrates that homology-dependent integration depends on a functional HR mechanism. On the other hand, as shown in ref. 11, HI was 100% and NHI was 0% in *mus-52*, suggesting that all NHI events depend on MUS-52 when foreign DNA carrying 2-kbp homology is introduced into wild type. Transformation frequency in *mus-52* ($3.81 \pm 0.39 \times 10^{-6}$) was almost the same as in wild type ($4.07 \pm 0.67 \times 10^{-6}$). However, in the NHI-defective mutant, homology-dependent integration events increased 4-fold over wild type. Conversely, the NHI frequency in HR-defective mutants, in which HI could not occur, increased significantly compared with wild type. These results suggest that pathways of HI and NHI compete against one another in wild-type cells.

Table 1. Integration frequency of an exogenous DNA fragment that has a 2-kbp *mtr* homologous sequence flanking the *bar* gene on both sides

Strain	*S. cerevisiae* homolog	TF ± SE,* $\times 10^{-6}$	Relative value of TF†	HI,‡ %	HI frequency,§ $\times 10^{-6}$	Relative value of HI frequency¶	NHI,‖ %	NHI frequency,** $\times 10^{-6}$	Relative value of NHI frequency††
Wild type		4.07 ± 0.67	1	23.33	0.95	1	76.67	3.12	1
mus-52	*YKU80*	3.81 ± 0.39	0.94	100	3.81	4.01	0	0	0
mus-11	*RAD52*	27.33 ± 6.33	6.71	0	0	0	100	27.33	8.76
mei-3	*RAD51*	29.83 ± 3.94	7.33	0	0	0	100	29.83	9.56
mus-25	*RAD54*	15.17 ± 2.47	3.73	0	0	0	100	15.17	4.86
mus-52 mus-11	*YKU80 RAD52*	0	0	0	0	0	0	0	0
mus-52 mei-3	*YKU80 RAD51*	0.32 ± 0.04	0.08	96.26	0.31	0.33	3.74	0.01	0.003
mus-52 mus-25	*YKU80 RAD54*	0.08 ± 0.03	0.02	88.9	0.07	0.07	11.1	0.009	0.003

TF, transformation frequency.

*Frequency was calculated as the number of bialaphos-resistant colonies per total cell number. Averages and standard errors are from more than three independent experiments.

†Relative value of transformation frequency was calculated as the transformation frequency in the mutant divided by the transformation frequency in the wild type.

‡HI (%) = (the number of PFP-resistant colonies/the number of bialaphos-resistant colonies) × 100.

§HI frequency = (the number of PFP-resistant colonies/the number of bialaphos-resisrant colonies) × transformation frequency.

¶Relative value of HI frequency was calculated as the HI frequency in the mutant divided by the HI frequency in the wild type.

‖NHI (%) = (the number of PFP-sensitive colonies/the number of bialaphos resistant colonies) × 100.

**NHI frequency = (the number of PFP-sensitive colonies/the number of bialaphos-resistant colonies) × transformation frequency.

††Relative value of NHI frequency was calculated as the NHI frequency in the mutant divided by the NHI frequency in the wild type.

Table 2. Integration frequency of an exogenous DNA fragment that has 50-bp *mtr* homologous sequence flanking the *bar* gene on both sides

Strain	*S. cerevisiae* homolog	TF ± SE,* $\times 10^{-6}$	Relative value of TF†	HI,‡ %	HI frequency,§ $\times 10^{-6}$	Relative value of HI frequency¶	NHI,‖ %	NHI frequency, ** $\times 10^{-6}$	Relative value of NHI frequency††
Wild type		17.25 ± 1.91	1	0.18	0.03	1	99.82	17.22	1
mus-52	*YKU80*	0.03 ± 0.01	0.0017	0	0	0	100	0.03	0.0017
mus-11	*RAD52*	125.2 ± 25.75	7.26	0	0	0	100	125.2	7.27
mei-3	*RAD51*	128.33 ± 15.9	7.44	0	0	0	100	128.33	7.45
mus-25	*RAD54*	124.4 ± 21.11	7.21	0	0	0	100	124.4	7.22
mus-52 mus-11	*YKU80 RAD52*	0	0	0	0	0	0	0	0
mus-52 mei-3	*YKU80 RAD51*	0.0025 ± 0.0025	0.00014	0	0	0	100	0.0025	0.00015
mus-52 mus-25	*YKU80 RAD54*	0.005 ± 0.0022	0.00029	0	0	0	100	0.005	0.00029

TF, transformation frequency.

*Frequency was calculated as the number of bialaphos-resistant colonies per total cell number. Averages and standard errors are from more than three independent experiments.

†Relative value of transformation frequency was calculated as the transformation frequency in the mutant divided by the transformation frequency in the wild type.

‡HI (%) = (the number of PFP-resistant colonies/the number of bialaphos-resistant colonies) × 100.

§HI frequency = (the number of PFP-resistant colonies/the number of bialaphos-resisrant colonies) × transformation frequency.

¶Relative value of HI frequency was calculated as the HI frequency in the mutant divided by the HI frequency in the wild type.

‖NHI (%) = (the number of PFP-sensitive colonies/the number of bialaphos resistant colonies) × 100.

**NHI frequency = (the number of PFP-sensitive colonies/the number of bialaphos-resistant colonies) × transformation frequency.

††Relative value of NHI frequency was calculated as the NHI frequency in the mutant divided by the NHI frequency in the wild type.

To further investigate the relationship between HI and NHI in the chromosome integration pathway, we examined the transformation frequency of the *mus-52 mus-11* double mutant, in which both NHEJ and HR are inactive. No transformants appeared, indicating that foreign DNA carrying 2 kbp of homology was not integrated in this double mutant (Table 1) and that the *RAD52* homolog *mus-11* and the *YKU80* homolog *mus-52* are absolutely required for integration of foreign DNA carrying 2 kbp of homology.

On the other hand, a small number of bialaphos-resistant colonies were still found in the *mus-52 mei-3* and the *mus-52 mus-25* double mutants, which are also defective in the functions of both HR and NHEJ. The majority of those colonies (96.26 and 88.9%, respectively) were resistant to PFP, meaning that they were derived from HI although the recipient strains were defective in HR. We also confirmed that *bar* was integrated at the *mtr* locus using PCR (data not shown). This finding suggests that a second HI pathway is activated when the two major chromosomal integration pathways, MUS-52-dependent NHI and MEI-3-dependent HI, are blocked. This putative second HI pathway must depend on MUS-11, because DNA fragments were not integrated into the chromosome at all in the *mus-52 mus-11* double mutant. Furthermore, transformation by NHI also occurred at a very low level in *mus-52 mei-3* and *mus-52 mus-25* (0.01×10^{-6} and 0.009×10^{-6}, respectively), suggesting the existence of a MUS-11-dependent but MUS-52-independent second NHI pathway for chromosomal integration.

With 50-bp homology (Table 2), the HI rate in wild type was extremely low (0.18%), indicating that 50 bp of homology is not enough for effective homology searching and targeting. HI was not increased even in *mus-52*. However, a low rate of NHI was detected in *mus-52*, which is defective in NHEJ function. This finding supports the existence of MUS-52-independent NHI. A similar effect was seen in *mus-52 mei-3* and *mus-52 mus-25* double mutants. We conclude that MUS-11 and MUS-52 are key regulators of integration in *Neurospora* and that there are four subpathways: two major pathways, one of which is MEI-3-dependent, governing HI, the other MUS-52-dependent, governing NHI, and two minor "back-up" pathways, one MEI-3-independent HI and the other MUS-52-independent NHI.

Characterization of the *Neurospora LIG4* Homolog, *mus-53*. To further study the mechanism of NHI by NHEJ, we searched the *Neurospora* genome database (www.broad.mit.edu/annotation/fungi/neurospora/) to find an ortholog of human *LIG4*. A candidate was identified that encodes a 1,046-aa polypeptide which shows 25% identity and 38% similarity to human Lig4. Furthermore, this protein has two tandem BRCA1 C-terminal domains at the C terminus, which are conserved in human Lig4 (19) and *S. cerevisiae* Dnl4/Lig4 (20). The BRCA1 C-terminal domains of DNA ligase IV in human and yeast are essential for binding to another NHEJ protein, Xrcc4 or Lif1, respectively (21, 22).

To investigate its function in *Neurospora*, we used gene replacement to disrupt the *LIG4* homolog as described in *Materials and Methods*. Mutagen sensitivity of the disrupted mutant was analyzed by spot test (Fig. 2*A*). The mutant showed mild sensitivity to methyl methanesulfonate (MMS) and bleomycin (BLM) but was not sensitive to UV or to other chemical agents. Following the established rules of genetic nomenclature in *Neurospora* (23), this gene was named *mus-53*. The gene maps near *leu-1* in linkage group IIIR. Apical growth of *mus-53* in race tubes was normal, and no morphological abnormalities were observed (data not shown). Homozygous crosses were fertile, with normal asci and ascospores.

Epistatic relationships between *mus-53* and other recombination repair genes were examined using double mutants with *uvs-6*, *mei-3*, *mus-11*, and *mus-52*, and determining the sensitivity of each strain to MMS (Fig. 2*B*). The *uvs-6* mutation (yeast *RAD50*) is epistatic to *mus-53*. In contrast, both the *mus-53 mei-3* and the *mus-53 mus-11* double mutants were more sensitive than either parental single mutant. Sensitivity of the *mus-53 mus-52* double mutant was identical to that of the parental *mus-53* strain. *mus-53* therefore belongs to the NHEJ group of recombination repair mutants and not to the HR group.

Highly Efficient Gene Targeting Is Observed in *mus-53*. Gene targeting was used to determine whether the gene targeting frequency was increased in *mus-53* as well as in *mus-52*. With 2-kbp homology, the targeting frequency was 100% in *mus-53*, the same as in *mus-52* (Table 3). However, transformation was five times less frequent than in wild type ($0.85 \pm 0.08 \times 10^{-6}$ vs. $4.07 \pm 0.67 \times 10^{-6}$), and this low transformation frequency was suppressed by *mus-52*. The low transformation frequency in *mus-53* might be explained if the repair pathway cannot subsequently be changed from NHI to HI once MUS-52 proteins start to work. This result suggests that

GENETICS

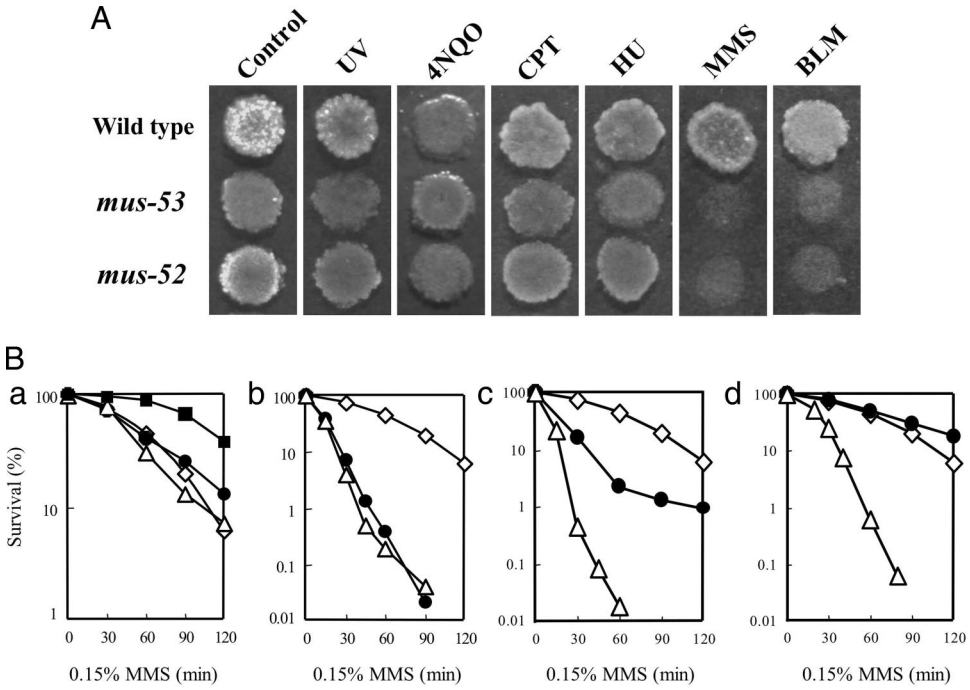

Fig. 2. Sensitivity and epistasis analysis of *mus-53*. (*A*) Sensitivity of wild type, *mus-52*, and *mus-53* to UV and chemical agents. Conidial suspension was spotted on the agar surface of plates containing 4-nitroquinoline 1-oxide (4NQO, 75 ng/ml), camptothecin (CPT, 0.4 μg/ml), hydroxyurea (HU, 1.5 mg/ml), MMS (0.175 μl/ml), and bleomycin (BLM, 5 μg/ml). Cells were UV-irradiated at 375 J/m^2. (*B*) Sensitivity to MMS of double mutants compared with their parental single mutants. A conidial suspension was treated with MMS (1.5 μl/ml) for the indicated time. (*a*) Wild type (filled squares), *mus-52* (filled circles), *mus-53* (open diamonds), and *mus-52 mus-53* (open triangles). (*b*) *mus-53* (open diamonds), *uvs-6* (filled circles), and *mus-53 uvs-6* (open triangles). (*c*) *mus-11* (filled circles), *mus-53* (open diamonds), and *mus-11 mus-53* (open triangles). (*d*) *mei-3* (filled circles), *mus-53* (open diamonds), and *mei-3 mus-53* (open triangles).

MUS-53 acts later than MUS-52 during gene integration. On the other hand, when foreign DNA with only 50-bp homology was introduced into *mus-53*, no transformants appeared. We hypothesize that MUS-53 is essential for integration of foreign DNA with short homology.

MUS-53 Is a Key Regulator of NHI. To test whether our hypothesis is correct, 2-kbp, 1-kbp, 500-bp, 300-bp, 100-bp, and 50-bp lengths of the *mtr* gene were attached on both sides of the *bar* gene and transformed into wild type, *mus-52*, and *mus-53*. Transformation frequency and the rate of gene targeting were assayed (Fig. 3). In wild type, the gene-targeting rate was low when the homology was short. HI was rare even with a homology length of 300 bp. In contrast, the gene-targeting rate in *mus-52* was ≈50% at 300-bp homology length, increasing to 100% with homology >1 kbp. In *mus-52*, both transformation frequency and gene-targeting rate were low when the homology was short, perhaps because the MUS-52-independent NHI pathway was activated by the short

Table 3. Integration frequency of an exogenous DNA fragment that has a 2-kbp (bold) or 50-bp (italic) *mtr* homologous sequence on both sides of *bar* gene in the *mus-53* mutant

Strain	*S. cerevisiae* homolog	TF ± SE,* ×10^{-6}	Relative value of TF†	HI,‡ %	HI frequency,§ ×10^{-6}	Relative value of HI frequency¶	NHI,‖ %	NHI frequency,** ×10^{-6}	Relative value of NHI frequency††
Wild type		**4.07 ± 0.67**	**1**	**23.33**	**0.95**	**1**	**76.67**	**3.12**	**1**
		17.25 ± 1.91	*1*	*0.18*	*0.03*	*1*	*99.82*	*17.22*	*1*
mus-52	*YKU80*	**3.81 ± 0.39**	**0.94**	**100**	**3.81**	**4.01**	**0**	**0**	**0**
		0.03 ± 0.01	*0.0017*	*0*	*0*	*0*	*100*	*0.03*	*0.0017*
mus-53	*LIG4*	**0.85 ± 0.08**	**0.21**	**100**	**0.85**	**0.89**	**0**	**0**	**0**
		0	*0*	*0*	*0*	*0*	*0*	*0*	*0*
mus-52 mus-53	*YKU80 LIG4*	**4.37 ± 0.29**	**1.07**	**100**	**4.37**	**4.6**	**0**	**0**	**0**

TF, transformation frequency. See Fig. 3 for the effect of intermediate-sized flanks.

*Frequency was calculated as the number of bialaphos-resistant colonies per total cell number. Averages and standard errors are from more than three independent experiments.

†Relative value of transformation frequency was calculated as the transformation frequency in the mutant divided by the transformation frequency in the wild type.

‡HI (%) = (the number of PFP-resistant colonies/the number of bialaphos-resistant colonies) × 100.

§HI frequency = (the number of PFP-resistant colonies/the number of bialaphos-resisrant colonies) × transformation frequency.

¶Relative value of HI frequency was calculated as the HI frequency in the mutant divided by the HI frequency in the wild type.

‖NHI (%) = (the number of PFP-sensitive colonies/the number of bialaphos resistant colonies) × 100.

**NHI frequency = (the number of PFP-sensitive colonies/the number of bialaphos-resistant colonies) × transformation frequency.

††Relative value of NHI frequency was calculated as the NHI frequency in the mutant divided by the NHI frequency in the wild type.

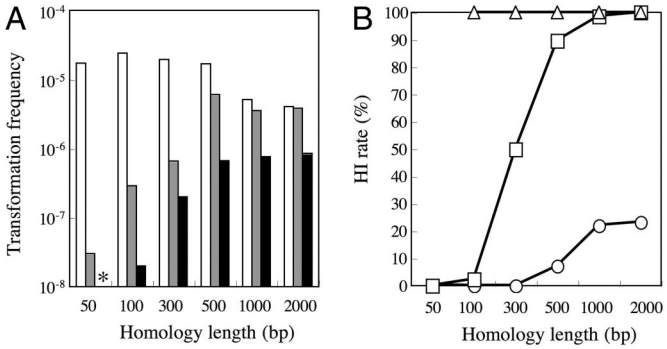

Fig. 3. Homology-dependent transformation frequency and HI in wild type, *mus-52*, and *mus-53*. Transformation frequency and HI were measured according to the strategy shown in Fig. 1. (*A*) Open bars, gray bars, and filled bars indicate transformation frequency in wild type, *mus-52*, and *mus-53* as recipients. (*B*) Open circles, open squares, and open triangles indicate rates of HI in wild type, *mus-52*, and *mus-53*, respectively. The asterisk indicates that there was no *mtr*-resistant transformant.

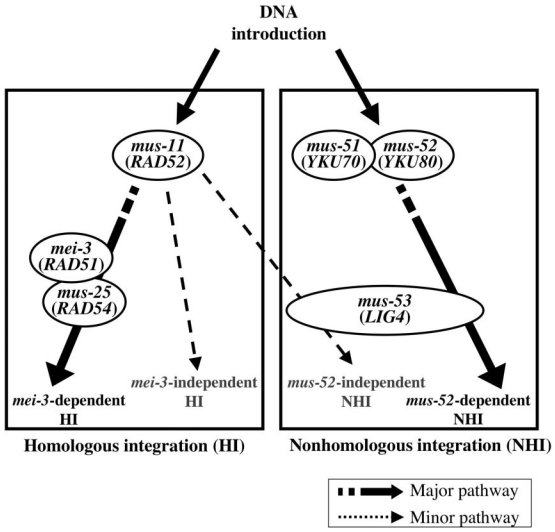

Fig. 4. Pathways for integration of exogenous DNA into chromosomal DNA. Exogenous DNA is integrated into the chromosomes by two major pathways, *mus-11*-dependent and *mus-52*-dependent. Downstream of these two chromosomal integration pathways is achieved by four pathways: two involving *mei-3*-dependent and *mei-3*-independent HI and two involving *mus-52*-dependent and *mus-52*-independent non-HI. Both nonhomologous integration pathways, *mus-52*-dependent and *mus-52*-independent, require *mus-53*. The genes in parentheses represent *S. cerevisiae* homologs.

homology even though integration could not occur via HR. Transformation frequency was lower in *mus-53* than in *mus-52* when homology was short. In *mus-53*, surprisingly, gene targeting was 100% even with 100-bp homology, but no transformants appeared with 50-bp homology. This means that 50-bp homology is not enough for gene targeting even in *mus-53*.

We conclude that MUS-53 function is required for all NHI pathways, both MUS-52-dependent and MUS-52-independent. Accordingly, DNA introduced into *mus-53* is integrated only at the target site.

Discussion

We demonstrated previously that gene-targeting efficiency becomes 100% in *Neurospora* mutants *mus-51* or *mus-52*, which are defective in end-joining (11). The first step in non-HR repair of DSBs is binding of Ku70 and Ku80 heterodimers to broken DNA ends. After the DNA ends are processed by Ku proteins, they are joined by the Lig4–Xrcc4 complex. Genetic characterization of *mus-53*, which is the *Neurospora* ortholog of human *LIG4*, indicated that Lig4 plays a significant role in NHI.

Targeting experiments showed distinct differences between *mus-52* and *mus-53*. In *mus-52*, transformation frequency was almost the same as in wild type, but in *mus-53* it was 4–5 times lower, as expected if HI frequency per total transformants is the same in *mus-53* as in the wild type, and the only transformants appearing on the selection plate are from HI. In a mutant defective in MUS-53 protein, all integrations are processed by the HR pathway.

Use of *mus-53* offers a distinct advantage when the transforming DNA has limited homology with the recipient sequence. When DNA with <500-bp homology is introduced into *mus-52*, HI decreases and NHI increases as homology length becomes shorter. In *mus-53*, however, transformants are exclusively from HI, even in experiments with short homology. This result is important because it means that with *mus-53* as recipient, all transformants will be from HI and none will be from NHI. The host is thus protected from NHI, and there is no need for further tedious experiments to determine whether DNA fragments are integrated ectopically. Although targeting has great promise for gene therapy, NHI has been a serious problem because it may activate protooncogenes and result in cancer. The system described here may provide a solution.

Four targeting patterns were observed in targeting experiments using three HR-deficient strains (*mei-3*, *mus-11*, and *mus-25*) and two NHEJ-deficient strains (*mus-52* and *mus-53*) (Fig. 4). Major transformation pathways are MEI-3-dependent HI and MUS-52-dependent NHI, whereas minor pathways are MUS-11-dependent but MEI-3-independent HI and MUS-11-dependent but MUS-52-independent NHI. MUS-51 and MUS-52 interact physically and are concerned in the same function (data not shown). The fact that no transformants appeared in the *mus-11 mus-52* double mutant means that only these two chromosomal-integration pathways are present.

In yeast, Rad51-dependent HR and Ku-Lig4-dependent NHEJ are major DSB repair pathways. At least three additional pathways have been reported: Ku-independent DSB rejoining, Rad52-dependent *s*ingle *s*trand *a*nnealing (SSA), and Rad52-dependent end-joining (24–26). We anticipate that these pathways exist and function in the minor integration pathway in *Neurospora*.

NHEJ-independent DSB rejoining has also been reported in mammals (27). However, the relationship between DSB repair and gene targeting is not clear. In the present study, we used *Neurospora* to demonstrate the importance of using a Lig4-deficient strain for

Table 4. Strains of *Neurospora crassa* used in this study

Strain/FGSC number	Genotype	Source/reference
C1-T10-37A	*A*	Laboratory stock
C1-T10-28a	*A*	Laboratory stock
74-OR31-16A	*A al-2 pan-2 cot-1*	(29)
54yo-828-3	*A mus-52::Hyg^r*	(11)
54yo-828-4	*a mus-52::Hyg^r*	(11)
FGSC6409A	*A mus-11*	FGSC
FGSC2764A	*A mei-3*	FGSC
FGSC6425a	*a mus-25*	FGSC
54yo-8m11-4	*A mus-52::Hyg^r mus-11*	This study
54yo-8m3-17	*A mus-52::Hyg^r mei-3*	(11)
54yo-8m25-13	*A mus-52::Hyg^r mus-25*	This study
FGSC10139A	*A mus-53::Hyg^r*	This study
FGSC10140a	*a mus-53::Hyg^r*	This study
ICBC480A	*A mus-52::Hyg^r mus-53::Hyg^r al-2*	This study
74OR-270-104a	*a uvs-6 al-2 pan-2 cot-1*	Laboratory stock
ICBC461a	*a mus-53::Hyg^r uvs-6 al-2 pan-2*	This study
ICBC422a	*a mus-53::Hyg^r mus-11 pan-2*	This study
ICBC436A	*A mus-53::Hyg^r mei-3 pan-2*	This study

FGSC, Fungal Genetics Stock Center.

GENETICS

gene targeting. Our results may provide a pathway for developing gene-targeting methods in higher eukaryotes.

Materials and Methods

Strains and Plasmids. Table 4 shows the *N. crassa* strains used in these experiments. C1-T10-34A, C1-T10-28a (28), and 74-OR31-16A (29) are wild-type strains. The *mus-53*::*Hyg*^{r} strain was generated by gene replacement as described (11); to make a targeting vector, 1.3-kbp EcoRV DNA of the central region of the *N. crassa LIG4* homolog, *mus-53* (NCU06264.2), was replaced by a 1.5-kbp length of the hygromycin-resistance gene (*Hyg*^{r}). The vector was introduced into wild-type 74-OR31-16A. Hygromycin-resistant transformants were isolated, and it was confirmed by PCR and Southern blotting whether a *mus-53* gene was disrupted correctly in those strains. The transformants were then backcrossed to wild-type C1-T10-28a to make the genetic background homogeneous. Strains KZM6220A (FGSC10139A) and KZM6224a (FGSC10140a) were used as *mus-53A* and *mus-53a* standards. *Escherichia coli* strains DH1 and XL-1 Blue were used for amplification of plasmids. Plasmids pUC19 (Stratagene, La Jolla, CA) and pGEM-T Easy (Promega, Madison, WI) were generally used for construction of new vectors. pBARGEM7-1 (30) carrying *bar* and pCSN43 (31) carrying *Hyg*^{r} were obtained from the Fungal Genetics Stock Center (University of Missouri, Kansas City, MO).

General Genetic Manipulation in *N. crassa*. Genetic analysis was carried out as described by Davis and de Serres (32).

Electroporation. Electroporation was used for introduction of exogenous DNA into recipient cells as described (11).

Determination of Transformation Frequency and Gene Targeting Rate. To measure integration frequency and the rate of targeting to the *mtr* locus, vector pGS1-2KR (9.5 kbp) was constructed as follows: A DNA fragment of *mtr* was generated by PCR using *N. crassa* genomic DNA as a template and the two primers: *mtr*-5′ (5′-GAAACGACGGGATGTGAGAT-3′) and *mtr*-3′ (5′-GATAATGAGGTAGCAGGAGC-3′). PCR cycling was carried out with the Expand High-Fidelity PCR system (Roche Diagnostics, Indianapolis, IN) following the manufacturer's protocol. The PCR product was integrated into pGEM-T Easy (Promega) to make pGEMMTR. Then it was digested with blunting enzyme MscI to delete a ~1-kbp fragment containing the promoter and part of the *mtr* ORF. A 2.7-kbp DNA fragment containing the bialaphos resistance gene *bar* was cut out from pBARKS1 with blunting enzymes ScaI and SmaI and inserted into MscI-digested pGEMMTR to produce pGS1-2KR, which carries 2 kbp of the *mtr* gene on both sides of *bar*. We also constructed pGS1-1KR, pGS1-500R, pGS1-300R, pGS1-100R, and pGS1-50R, which have 1 kbp, 500 bp, 300 bp, 100 bp, or 50 bp of *mtr* on both sides of *bar*, respectively. Digestion of these plasmids with EcoRI produces 6.7-kbp, 4.7-kbp, 3.7-kbp, 3.3-kbp, 2.9-kbp, and 2.8-kbp linear fragments carrying 2 kbp, 1 kbp, 500 bp, 300 bp, 100 bp, or 50 bp of *mtr* on both sides of *bar*, respectively. These fragments were introduced into various host strains by electroporation. Conidial suspensions were then plated on medium containing bialaphos (200 μg/ml) and incubated at 30° for 3 days. Transformants resistant to bialaphos were isolated and tested by spot tests for resistance to PFP (20 μg/ml) and to bialaphos. To confirm whether transformants included products of HI, PCR with two primer sets was performed as described (11).

Mutagen Sensitivity. Sensitivity was investigated by spotting a conidial suspension on agar medium containing the chemical agent (33). Sensitivity to MMS was determined as described (34).

This work was supported by Rational Evolutionary Design of Advanced Biomolecules, Saitama Prefecture Collaboration of Regional Entities for the Advancement of Technological Excellence, Japan Science and Technology Agency.

1. Haber J (2000) *Trends Genet* 16:259–264.
2. Critchlow SE, Jackson SP (1998) *Trends Biochem Sci* 23:394–398.
3. Teo, S-H., Jackson SP (1997) *EMBO J* 16:4788–4795.
4. Adachi N, Ishino T, Ishii Y, Takeda S, Koyama H (2001) *Proc Natl Acad Sci USA* 98:12109–12113.
5. Daley JM, Palmbos PL, Wu D, Wilson TE (2005) *Annu Rev Genet* 39:431–451.
6. Check E (2002) *Nature* 420:116–118.
7. Hacein-Bey-Abina S, Von Kalle C, Schmidt M, McCormack MP, Wulffraat N, Leboulch P, Lim A, Osborne CS, Pawliuk R, Morillon E, *et al.* (2003) *Science* 302:415–419.
8. Hatakeyama S, Ishii C, Inoue H (1995) *Mol Gen Genet* 249:439–446.
9. Sakuraba Y, Schroeder AL, Ishii C, Inoue H (2000) *Mol Gen Genet* 264: 392–401.
10. Handa N, Noguchi Y, Sakuraba Y, Ballario P, Macino G, Fujimoto N, Ishii C, Inoue H (2000) *Mol Gen Genet* 264:154–163.
11. Ninomiya Y, Suzuki K, Ishii C, Inoue H (2004) *Proc Natl Acad Sci USA* 101:12248–12253.
12. Colot HV, Park G, Turner GE, Ringelberg C, Crew CM, Litvinkova L, Weiss RL, Borkovich KA, Dunlap JC (2006) *Proc Natl Acad Sci USA* 103:10352–10357.
13. Nayak T, Szewczyk E, Oakley CE, Osmani A, Ukil L, Murray SL, Hynes MJ, Osmani SA, Oakley BR (2006) *Genetics* 172:1557–1566.
14. da Silva Ferreira ME, Kress MR, Savoldi M, Goldman MH, Hartl A, Heinekamp T, Brakhage AA, Goldman GH (2006) *Eukaryotic Cell* 5:207–211.
15. Krappmann S, Sasse C, Brous GH (2006) *Eukaryotic Cell* 5:212–215.
16. Takahashi T, Masuda T, Koyama Y (2006) *Mol Genet Genomics* 275:460–470.
17. Goins CL, Gerik KJ, Lodge JK (2006) *Fungal Genet Biol* 43:531–544.
18. DeBusk RM, Debusk AG (1980) *J Bacteriol* 143:188–197.
19. Grawunder U, Wilm M, Wu X, Kulesza P, Wilson TE, Mann M, Lieber MR (1997) *Nature* 388:428–429.
20. Wilson TE, Grawunder U, Lieber MR (1997) *Nature* 388:495–498.
21. Dore AS, Furnham N, Davies OR, Sibanda BL, Chirgadze DY, Jakson SP, Pellegrini L, Blundell TL (2006) *DNA Repair* 7:362–368.
22. Critchlow SE, Bowater RP, Jackson SP (1997) *Curr Biol* 7:588–598.
23. Perkins DD, Radford A, Sachs MS (2001) *The* Neurospora *Compendium* (Academic, New York).
24. Ma JL, Kim EM, Haber JE, Lee SE (2003) *Mol Cell Biol* 23:8820–8828.
25. Yu X, Gabriel A (2003) *Genetics* 163:843–856.
26. Daley JM, Wilson TE (2005) *Mol Cell Biol* 25:896–906.
27. Wang H, Perrault AR, Takeda Y, Qin W, Wang H, Iliakis G (2003) *Nucleic Acids Res* 31:5377–5388.
28. Tamaru H, Inoue H (1989) *J Bacteriol* 171:6288–6293.
29. de Serres FJ, Inoue H, Schupbach ME (1980) *Mutation Res* 71:53–65.
30. Pall ML, Brunelli JP (1993) *Fungal Genet Newslett* 40:59–62.
31. Staben C, Jensen B, Singer M, Pollock J, Schechman M, Kinsey J, Selker E (1989) *Fungal Genet Newslett* 36:79–81.
32. Davis RH, de Serres FJ (1970) *Methods Enzymol* 17:79–143.
33. Kato A, Akamatsu Y, Sakuraba Y, Inoue H (2004) *Curr Genet* 45:37–44.
34. Inoue H, Ishii C (1984) *Mutation Res* 125:185–194.